Modeling the Impact of Human Population on the Dynamics of Atmospheric Carbon Dioxide and Climate Change

Rabindra Kumar Gupta

Department of Mathematics, Butwal Multiple Campus, Tribhuvan University, Butwal, 284403, Lumbini, Nepal

Correspondence to: Rabindra Kumar Gupta, Email:gupta.rabindra04@gmail.com

Abstract: *A non-linear model is put forward and comprehended to understand climate change caused by change in the most abundance greenhouse gas Carbon Dioxide (CO_2) due to the influence of human activities. The deterministic model (ODE) is followed by stochastic model (SDE) with the introduction of random noise to depict the more realistic situation as it includes environmental disturbances. Three state variables which are used in the model are human population, concentration of CO_2, and forest biomass. It is formulated on the assumption that the concentration of atmospheric CO_2 increases due to anthropogenic emissions as well as naturally when organisms respire, forest fire and volcano eruption. It also depletes naturally through natural sink (ocean, soil and plants). Equilibrium analysis and stability analysis of the model are performed. Numerical simulations are performed to justify the analytical results. The outcomes of the paper explain that the concentration of atmospheric CO_2 can be lowered by minimizing the rate of use of forest biomass which in turn slows down the growth of human population that ultimately reduces the anthropocentric emissions of CO_2 gas. This decrement in the concentration of atmospheric CO_2 gas controls the climate change.*

Keywords: Human population, CO_2 gas, Climate change, Stability, Forest biomass

1 Introduction

Carbon dioxide (CO_2) gas is very crucial among greenhouse gases due to its prominent presence in the atmosphere [10]. Its atmospheric concentration has been progressively rising along with rising CO_2 emission, Figure(1). Research reveals that the average carbon dioxide level escalated from 418.05 ppm (parts per million) in March 2022 to 420.13 ppm in March 2023 [17]. The escalation in CO_2 level stands as a significant instigator of worldwide climate shifts, predominantly propelled by human actions like the combustion of fossil fuels (coal, oil, and natural gas) to generate energy, deforestation, and various industrial procedures. These practices emit substantial quantities of CO_2 and other greenhouse gases into the air, creating a heat-trapping effect that culminates in global warming. If the current upward trajectory of atmospheric CO_2 persists, it is highly probable that significant climatic shifts will transpire. These shifts could have far-reaching consequences for both human health and ecosystems. Additionally, the altered climate patterns are expected to influence the prevalence of various vector-borne illnesses such as dengue and malaria [6, 15]. Consequently, an imperative lies in comprehensively investigating the behavior of CO_2 gas within the atmosphere. This entails discerning the primary contributors to its presence and understanding their roles in driving changes in atmospheric CO_2 levels. Both the human population and forest biomass significantly contribute to the behavior of atmospheric CO_2 gas. The ever-growing population necessitates various developments, such as housing complexes, agricultural expanses, and transportation routes like roads. These demands for land are often met through deforestation, which leads to a persistent decline in forest biomass. This degradation of forest resources is primarily driven by the imperative to accommodate the expanding human population. Consequently, human-induced deforestation stands as a pivotal factor influencing alterations in atmospheric CO_2 levels [14]. It is found that one percent increase in human population causes about 1.42% increase in CO_2 gas [12]. Alexiadis [1] put forth a model aimed at scrutinizing the impact of human activities on the emission of CO_2. The outcome of the study led to the conclusion that anthropogenic CO_2 stands as the chief driving factor behind the phenomenon of global warming. Multiple studies have demonstrated a correlation between the rise in human population and an escalation in deforestation rates [2, 3, 7]. Conversely, forest biomass plays a vital role by capturing

and storing atmospheric carbon dioxide through the photosynthesis process. This not only mitigates the levels of CO_2 in the atmosphere but also contributes to the global efforts against climate change. Forest biomass significantly impacts the intricate dynamics of atmospheric carbon dioxide. Tennakone [13] has proposed and analyzed a model to study the biomass-carbon dioxide system. The outcomes of this study reveal that biomass-carbon dioxide equilibrium destabilizes due to immoderate deforestation. Panja [11]has introduced and scrutinized a model aimed at investigating the repercussions of global warming on the population. The findings of the study indicate that the instability of the system is exacerbated by the rise in global warming resulting from increased deforestation. To restore stability, the study suggests implementing various strategies to enhance the growth rate of forest biomass. One proposed solution is the initiation of a plantation program to alleviate the concentration of CO_2 in the atmosphere. Misra and Jha [9] have developed a model to assess the impact of deploying renewable energy sources on the future concentration of atmospheric CO_2. The primary objective of the study is to evaluate the potential effects of renewable energy sources in mitigating CO_2 levels. Their results demonstrate a substantial decrease in atmospheric CO_2 levels with the deployment of renewable energy sources. The system exhibits instability for low values of renewable energy growth, while stability is achieved for higher values of growth. In this paper, a model to study the impact of human population and forest biomass on the atmospheric concentration of CO_2 is formulated. The assumption is that increasing human population density results in deforestation for developmental purposes, ultimately reducing the carrying capacity of forest biomass. The model is constructed in reference to the framework introduced by Misra and Jha [8] who investigated the effects of population pressure on CO_2 dynamics. The paper is organized as follows, in the following section a mathematical model is presented, in section 3 mathematical analysis of the model is done, the condition for the feasibility of equilibria, and their stability analysis are carried out. In section 4 stochastic analogue of deterministic model is presented incorporating drift and diffusion terms to visualize randomness. Section 5 consists of numerical simulation to validate analytical findings and the paper ends with the conclusion in Section 6.
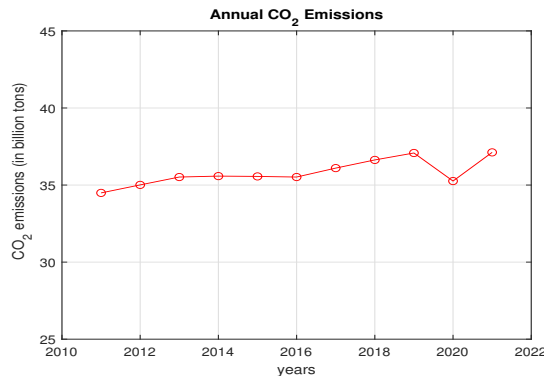

Figure 1: Amount of CO_2 emission. (Source: Global Carbon Project (2023))

2 The Mathematical Model

Table 1: Description of the state variables used in model.

Variables	Description
C_c	Concentration of CO_2 gas in the environment
H_n	Number of human population in the region
B_f	Forest biomass

The model formulation incorporates dynamical variables of the region, as outlined in the Table (1). Atmospheric CO_2 increases naturally (e.g.; volcanic eruption, respiration process of living organism etc.) at

a consistent rate denoted as q. Additionally, there is anthropogenic emission at the rate γ, linked to human population since these emission arise from human activities such as clearing land for agriculture and development release CO_2 when trees are burned, emission of CO_2 from vehicles, ships and planes, burning fossils fuels releases CO_2 etc. The concentration of CO_2 depletes naturally (eg; photosynthesis by plants, natural sinks in the ocean) at the rate γ_0. It is considered that the human population grows logistically with an intrinsic growth rate r and carrying capacity K whereas the fossil biomass at the constant rate b. It is also assumed that the growth of forest biomass declines due to human population (human population clears forest for housing, agriculture etc.) at the rate α which in turn increase the population shown in the model with the factor $\alpha_1 \alpha H_n B_f$, where, α_1 is much less than 1, as human population gets foods or resources directly or indirectly from the forest biomass. Many individuals from developing countries tend to migrate back to their native homes after retirement, where energy consumption and industrialization levels are significantly lower. These areas typically rely on local materials, basic agricultural practices, and limited infrastructure, resulting in almost negligible carbon output. Therefore, the migration rate r_0, with $r >> r_0$ is considered to account for this negligible CO_2 emission. Forests are subjected to the various natural disturbances such as insect outbreaks, disease outbreak and seasonal variations (wind storms, ice storm). Furthermore, trees and plants have natural life spans, and as they age, their biomass gradually decrease (natural tree mortality). Also some trees species and plants decline while competing for resources such as sunlight , water and nutrients (competitive succession) leading to natural depletion of their biomass. Therefore, in the model it is taken that the Fossil biomass depletes naturally at the rate α_0. With the above assumptions the proposed model is given as,

$$
\begin{aligned}
\frac{dC_c}{dt} &= q + \gamma H_n - \gamma_0 C_c \\
\frac{dH_n}{dt} &= r H_n \left(1 - \frac{H_n}{K}\right) + \alpha_1 \alpha H_n B_f - r_0 H_n \\
\frac{dB_f}{dt} &= b - \alpha H_n B_f - \alpha_0 B_f
\end{aligned}
\tag{1}
$$

with the initial condition $C_c(0) > 0$, $H_n(0) \geq 0$, and $B_f(0) \geq 0$.

3 Mathematical Analysis

3.1 Positivity and boundedness

Theorem 3.1. *For all positive initial conditions, every solution of the model system* (1) *in* $\mathbb{R}_+^3$ *remains positive* $\forall\ t > 0$.

Proof. Right hand side of system (1) is continuous and locally Lipschitz in $\mathbb{R}_+^3$, so the system has unique solution on $[0, \tau)$, where $0 < \tau \leq +\infty$. Second equation of the system (1) by using Lemma 4 in [16] gives

$$
H_n(t) = H_n(0)\ exp\ \left[\int_0^t \left(r\left(1 - \frac{H_n(u)}{K}\right) + \alpha_1 \alpha B_f(u) - r_0\right) du\right] > 0.
$$

Now we want to show that $C_c(t) > 0\ \forall\ t \in [0, \tau)$. If this inequality does not hold then $\exists\ t_1 \in [0, \tau)$ such that $C_c(t_1) = 0$, $\frac{dC_c(t_1)}{dt} \leq 0$ and $C_c(t) > 0, \forall t \in [0, t_1)$. But from the first equation of system (1),

$$
\left.\frac{dC_c(t)}{dt}\right|_{t=t_1} = q + \gamma H_n(t_1) - \gamma_0 C_c(t_1) = q + \gamma H_n(t_1) > 0,
$$

contradicts $\frac{dC_c(t_1)}{dt} \leq 0$. So, $C_c(t) > 0\ \forall t \in [0, \tau)$. Similarly if $B_f(t) > 0$ is not correct then $\exists\ t_2 \in [0, \tau)$ such that $B_f(t_2) = 0$, $\frac{dB_f(t_2)}{dt} \leq 0$, and $B_f(t) > 0, \forall t \in [0, t_2)$. Furthermore, from the third equation of the model system (1), we obtain, $\left.\frac{dB_f(t)}{dt}\right|_{t=t_2} = b > 0$, contradicting $\frac{dB_f(t_2)}{dt} \leq 0$. Therefore, $B_f(t) > 0\ \forall t \in [0, \tau)$. $\qquad\square$

Theorem 3.2. *The domain within which each solution originating from the positive octant of the model system (1) remains bounded can be described as follows:*

$$\Gamma = \left\{ (C_c, H_n, B_f) \in \mathbb{R}_+^3 : 0 \leq C_c(t) \leq \frac{rq + \gamma K(r - r_0)}{r\gamma_0}, \ 0 \leq H_n(t) \leq \frac{K(r - r_0)}{r}, \right.$$
$$\left. 0 \leq B_f(t) \leq \frac{br}{\alpha K(r - r_0) + r\alpha_0} \right\},$$

The region Γ is closed and bounded in positive cone of three dimensional space.

Proof. From the second equation of the system (1), we have

$$\frac{dH_n}{dt} \geq (r - r_0)H_n - \frac{rH_n^2}{K}.$$

On solving the above differential equation, we get

$$\frac{1}{H_n(t)} \geq \frac{r}{K(r - r_0)} + Ce^{-(r - r_0)t},$$

which gives

$$\lim_{t \to \infty} \sup \frac{1}{H_n(t)} \geq \frac{r}{K(r - r_0)}.$$

Hence for any time $t > 0$,

$$0 \leq H_n(t) \leq \frac{K(r - r_0)}{r}.$$

Also from the first equation, using $H_n(t)$, we have

$$\frac{C_c(t)}{dt} + \gamma_0 C_c(t) \leq q + \frac{\gamma K(r - r_0)}{r}.$$

Solving using theory of differential inequality, we have

$$\lim_{t \to \infty} \sup C_c(t) \leq \frac{rq + \gamma K(r - r_0)}{r\gamma_0},$$

This implies

$$0 \leq C_c(t) \leq \frac{rq + \gamma K(r - r_0)}{r\gamma_0}.$$

Again from the third equation, we have

$$\frac{dB_f(t)}{dt} \leq b - \left(\alpha_0 + \frac{bK(r - r_0)}{r} \right) B_f(t).$$

By using theory of differential inequality, we have

$$\lim_{t \to \infty} \sup B_f(t) \leq \frac{br}{r\alpha_0 + \alpha K(r - r_0)}.$$

This gives

$$0 \leq B_f(t) \leq \frac{br}{r\alpha_0 + \alpha K(r - r_0)}.$$

$\square$

3.2 Feasibility of equilibria

The system has two equilibria: human population free equilibrium $X_{hfe} = \left(\dfrac{q}{\gamma_0}, 0, \dfrac{b}{\alpha_0}\right)$ and interior equilibrium $X_{ie} = (C_c^i, H_n^i, B_f^i)$. The equilibrium X_{hfe} is always feasible in the system and the existence of interior equilibrium is justified from the following analysis.

The second equilibrium equation of the system (1) gives

$$H_n = \frac{K(r - r_0 + \alpha\alpha_1 B_f)}{r} \equiv f(B_f(t)). \tag{2}$$

And from the third equilibrium equation, we have

$$H_n = \frac{b}{\alpha B_f} - \frac{\alpha_0}{\alpha} \equiv g(B_f(t)). \tag{3}$$

The curve $f(B_f(t))$ intersects the H_n and B_f axis at the points $\left(0, \dfrac{K(r - r_0)}{r}\right)$ and $\left(\dfrac{-(r - r_0)}{\alpha\alpha_1}, 0\right)$ respectively. Further $\dfrac{df}{dB_f} > 0$, so the curve $f(B_f(t))$ is an increasing function of $B_f(t)$ in the domain of definition Γ. Also, the curve $g(B_f(t))$ passes through the point $\left(\dfrac{-b}{\alpha_0}, 0\right)$ and is decreasing function of $B_f(t)$ since $\dfrac{dg}{dB_f} < 0$. These two curves intersect at unique point (B_f^i, H_n^i) if $b > \dfrac{\alpha_0(r - r_0)}{\alpha\alpha_1}$ in the interior of the positive quadrant. Corresponding to these values, a positive value C_c^i from the first equilibrium equation of the system (1) can be readily acquired. Thus the feasibility of interior equilibrium $X_{ie} = (C_c^i, H_n^i, B_f^i)$ of the system (1) is justified in Figure (2).
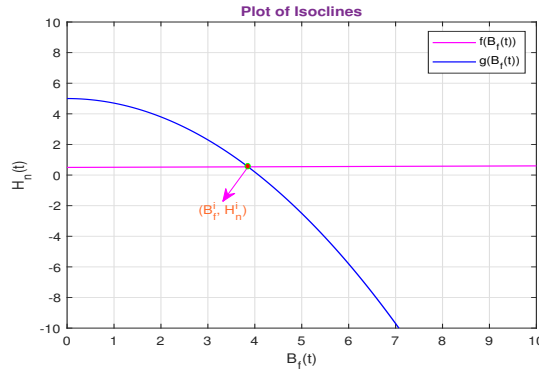

Figure 2: Plot of isoclines (10) and (3) intersecting at a positive point (B_f^i, H_n^i).

3.3 Stability analysis

In this section, our focus shifts towards investigating the impact of minor disturbances on equilibrium solutions and how they influence the behavior of the solutions within the context of system (1). The system's Jacobian matrix, crucial to our analysis, is as follows.

$$J = \begin{bmatrix} -\gamma_0 & \gamma & 0 \\ 0 & r\left(1 - \frac{2H_n}{K}\right) + \alpha\alpha_1 B_f - r_0 & \alpha\alpha_1 H_n \\ 0 & -\alpha B_f & -(\alpha H_n + \alpha_0) \end{bmatrix}$$

The Jacobian matrix at human population free equilibrium is

$$J_{X_{hfe}} = \begin{bmatrix} -\gamma_0 & \gamma & 0 \\ 0 & \left(r - r_0 + \frac{\alpha\alpha_1 b}{\alpha_0}\right) & 0 \\ 0 & \frac{\alpha b}{\alpha_0} & -\alpha_0 \end{bmatrix}$$

The eigenvalue $\left(r - r_0 + \frac{\alpha\alpha_1 b}{\alpha_0}\right)$ of the matrix $J_{X_{hfe}}$ is always positive as $(r - r_0) > 0$, so X_{hfe} is always unstable. The Jacobian matrix at interior equilibrium is,

$$J_{X_{ie}} = \begin{bmatrix} -\gamma_0 & \gamma & 0 \\ 0 & -\frac{rH_n^i}{K} & \alpha\alpha_1 H_n^i \\ 0 & -\alpha B_f^i & -(\alpha H_n^i + \alpha_0) \end{bmatrix}$$

One eigenvalue of the Jacobian matrix $J_{X_{ie}}$ is $-\gamma_0$ and the remaining two are obtained from the roots of the equation,

$$\lambda^2 + c_1\lambda + c_2 = 0, \tag{4}$$

where

$$c_1 = \frac{rH_n^i}{K} + \alpha H_n^i + \alpha_0$$

$$c_2 = \frac{rH_n^i}{K}(\alpha H_n^i + \alpha_0) + \alpha^2\alpha_1 H_n^i B_f^i.$$

Since $c_1, c_2 > 0$, Routh-Hurwitz criterion deduces that the roots of (4) are either real negative or complex with negative real component. Consequently, all three eigenvalues of the matrix $J_{X_{ie}}$ possess negative real components. This establishes that the interior equilibrium is endowed with local asymptotic stability.

Theorem 3.3. *The human population free equilibrium X_{hfe} always exists in the system and is always unstable in H_n direction, but the interior equilibrium X_{ie} exists if $b > \dfrac{\alpha_0(r - r_0)}{\alpha\alpha_1}$, and is locally asymptotically stable in the domain of definition Γ.*

3.4 Global stability analysis of X_{ie}

Theorem 3.4. *The interior equilibrium X_{ie}, if feasible, achieves globally asymptotic stability within its region of attraction if the condition outlined in (5) is satisfied*

$$9b^2 K^2 \alpha_1^2 \alpha^4 < 4(\alpha H_n^i + \alpha_0)^2(\alpha K(r - r_0) + r\alpha_0)^2. \tag{5}$$

Proof. A Lyapunov function is defined as

$$\mathcal{L} = \left[H_n - H_n^i - H_n^i ln\left(\frac{H_n}{H_n^i}\right)\right] + \frac{m_1}{2}(C_c - C_c^i)^2 + \frac{m_2}{2}(B_f - B_f^i)^2,$$

where, $m_1, m_2 > o$ are appropriately chosen. Differentiating $\mathcal{L}$ with respect to time t along the solution of the system, we get

$$\begin{aligned} \frac{d\mathcal{L}}{dt} &= -\frac{r}{K}(H_n - H_n^i)^2 - m_1\gamma_0(C_c - C_c^i)^2 - m_2(\alpha H_n^i + \alpha_0)(B_f - B_f^i)^2 \\ &\quad + \alpha\alpha_1(H_n - H_n^i)(B_f - B_f^i) + m_1\gamma(C_c - C_c^i)(H_n - H_n^i) \\ &\quad - m_2\alpha B_f(H_n - H_n^i)(B_f - B_f^i), \\ &= \left[-\frac{r}{3K}(H_n - H_n^i)^2 + \alpha\alpha_1(H_n - H_n^i)(B_f - B_f^i) - \frac{m_2}{2}(\alpha H_n^i + \alpha_0)(B_f - B_f^i)^2)\right] \\ &\quad + \left[-\frac{r}{3K}(H_n - H_n^i)^2 + m_1\gamma(C_c - C_c^i)(H_n - H_n^i) - m_1\gamma_0(C_c - C_c^i)^2\right] \\ &\quad + \left[-\frac{r}{3K}(H_n - H_n^i)^2 - m_2\alpha B_f(H_n - H_n^i)(B_f - B_f^i) - \frac{m_2}{2}(\alpha H_n^i + \alpha_0)(B_f - B_f^i)^2\right]. \end{aligned}$$

$\frac{d\mathcal{L}}{dt} < 0$ if the following inequalities hold.

$$m_1\gamma^2 < \frac{2}{3}\frac{r\gamma_0}{K}, \tag{6}$$

$$(\alpha\alpha_1)^2 < \frac{4}{3}\frac{r(\alpha H_n^i + \alpha_0)m_2}{K}, \tag{7}$$

$$\frac{m_2(\alpha b r)^2}{(\alpha K(r - r_0) + r\alpha_0)^2} < \frac{2}{3}\frac{r(\alpha H_n^i + \alpha_0)}{K}. \tag{8}$$

From the equation (6) choosing the value of $m_1 = \dfrac{r\gamma_0}{K\gamma^2}$ and from the (7) and (8), we have

$$\frac{3}{2}\frac{K(\alpha\alpha_1)^2}{r(\alpha H_n^i + \alpha_0)} < m_2 < \frac{2}{3}\frac{(\alpha H_n^i + \alpha_0)(\alpha K(r - r_0) + r\alpha_0)^2}{rK\alpha^2 b^2}. \tag{9}$$

From the inequality (9), the inequality (5) is obtained. $\qquad\square$

4 Stochastic Model

Deterministic models operate based on specific, quantitative characteristics of systems, without considering their probabilistic nature. They are particularly useful in situations where there are relatively few sources of uncertainty within the system. In practice, deterministic models often approximate real processes by using averaged probabilistic characteristics, such as estimating the average concentration of a pollutant instead of the actual concentration. These models are not influenced by random fluctuations or unexpected events. On the other hand, stochastic models address the probabilistic characteristics of systems and the processes they study. Due to random influences in the environment, identical initial conditions and input factors can lead to different outcomes that resemble the characteristic of a stochastic process. Stochastic models are better suited for capturing the uncertainty and variability inherent in real-world scenarios. Since the environment is often filled with randomness, the smooth depiction provided by deterministic models is inadequate for representing reality. To account for environmental fluctuations, system of stochastic differential equations (SDEs), which include drift and diffusion terms, is proposed. Thus the stochastic analogue of deterministic model system (1) is:

$$
\begin{aligned}
dC_c(t) &= (q + \gamma H_n - \gamma_0 C_c)dt - \sigma_1 C_c dB_1(t), \\
dH_n(t) &= \left(rH_n\left(1 - \frac{H_n}{K}\right) + \alpha_1\alpha H_n B_f - r_0 H_n\right)dt - \sigma_2 H_n dB_2(t), \\
dB_f(t) &= (b - \alpha H_n B_f - \alpha_0 B_f)dt - \sigma_3 B_f dB_3(t).
\end{aligned}
\tag{10}
$$

where $B_i's$ are one dimensional independent Brownian motions, $\sigma_i's$ are diffusion coefficients, representing the intensity of random fluctuations, and $dB_i(t)'s$ are the increment of the weiner process, representing the random fluctuation of Brownian motion.

5 Numerical Simulations

In this section the analytical findings are justified through numerical simulations using MATLAB 2018 and MATLAB $ode45$ function to solve the ODE system. It is based on an explicit Runge-Kutta method, which is a type of variable step method known for its efficiency and accuracy. The description of the parameters and their values for the purpose of numerical simulation is given in the Table (2). The set of values in the Table (2) is used throughout the simulations unless otherwise stated. The condition of existence of interior equilibrium is satisfied for the above values and we get positive values of all the state variables of the model system (1) and the eigenvalues of the matrix $J_{X_{ie}}$ are -0.0030, -0.00999 and -0.2000378893, which are all negative so the interior equilibrium X_{ie} is asymptotically stable. Figure(3) plots the variation of different state variables of the system (1) with respect to time for various values of reduction rate in forest biomass due to the interaction of human population. It is clear from the figure that both the concentration of atmospheric CO_2 gas and human population increase (decrease) with the increase (decrease) in the reduction rate of forest biomass α whereas forest biomass decreases as α increases. This indicates that the atmospheric CO_2 can be minimized, which in return controls the climate change by decreasing reduction rate of forest biomass due to human population. Figure (4) shows the atmospheric concentration of CO_2

Table 2: Parameters description with their values used for numerical simulations.

Parameters	Description	Values
q	Natural emission rate of CO_2 gas	1 ppm $month^{-1}$
b	Growth rate of forest biomass	0.2 ton $month^{-1}$
γ	Anthropogenic emission rate of CO_2 gas	0.05 ppm $person^{-1}month^{-1}$
γ_0	Depletion rate of CO_2 gas in the environment	0.003 $month^{-1}$
α	Rate of reduction in forest biomass due to human pop^n	0.0002 $person^{-1}month^{-1}$
α_0	Natural depletion of forest biomass	0.0002 $month^{-1}$
α_1	Growth of human population due to forest biomass	0.01 persons $month^{-1}$
r	Intrinsic growth rate of human population	0.01 $month^{-1}$
r_0	Migration rate of human pop^n from a region of high to low energy consumption and industrialization	0.00001 $month^{-1}$
K	Half saturation constant	1000 persons
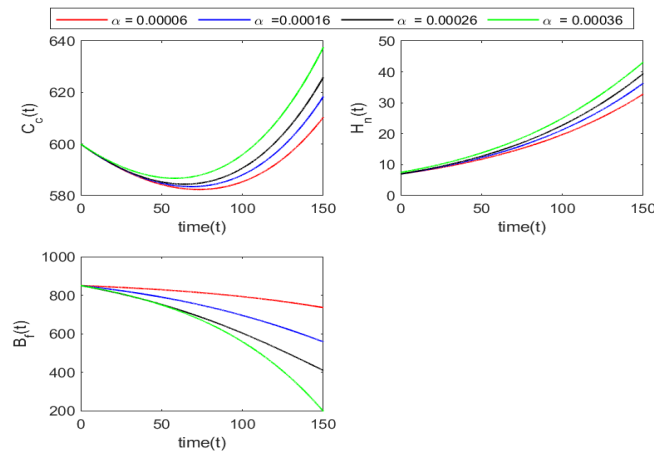
Figure 3: Variation plots of C_c, H_n and B_f for the system (1) for different values of α.
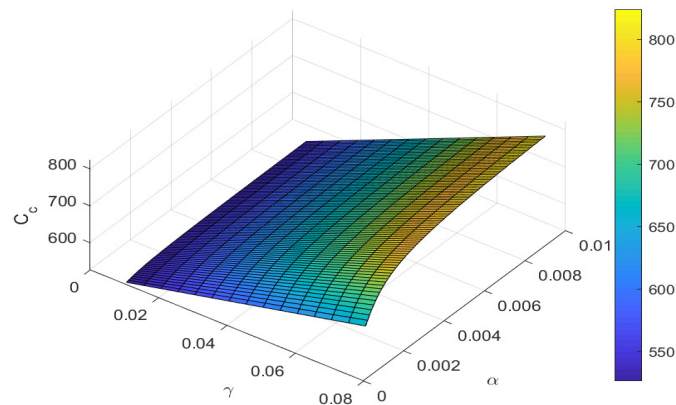
Figure 4: Surface plot showing the change in C_c for the system (1) with respect to α and γ.

gas plotted against the simultaneous change in the value of anthropogenic emission rate of CO_2 and reduction rate of forest biomass. The diagram reflects that atmospheric concentration of CO_2 increases with the increase in the reduction rate of forest biomass and rate of anthropogenic emission. From the surface plot in Figure (5) it is clear that the human population decreases (increases) with the decrease (increase) in both reduction rate of forest biomass and the carrying capacity of human population. The
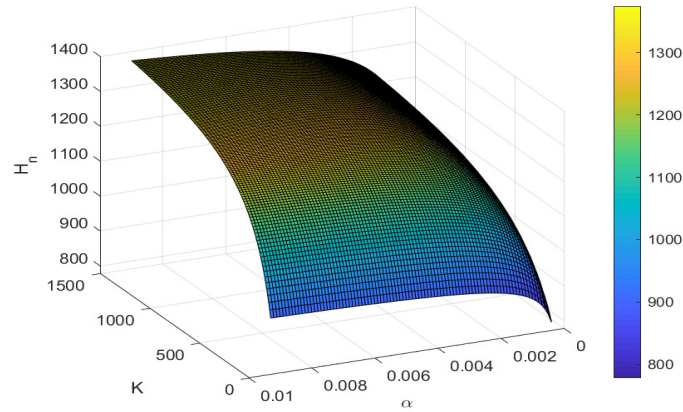
Figure 5: Surface plot reflecting the change in the human population H_n for the system (1) for different values of α and K.
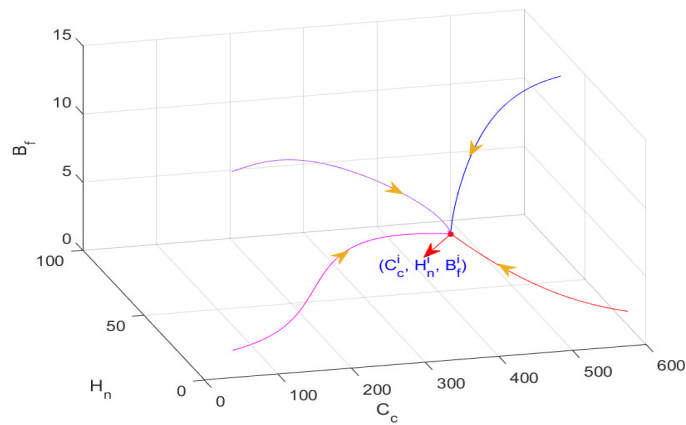

Figure 6: Global plot in the $C_c - H_n - B_f$ space for the system (1), the value of parameters are same as in the Table (2) except $\alpha = 0.00002$, $\alpha_1 = 0.0001$, and $\gamma = 0.005$.
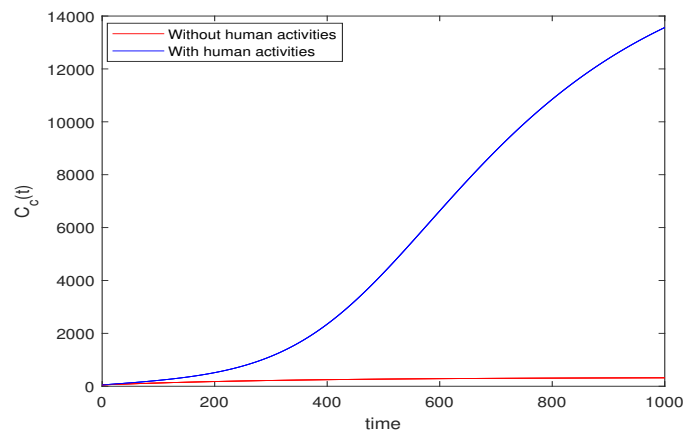

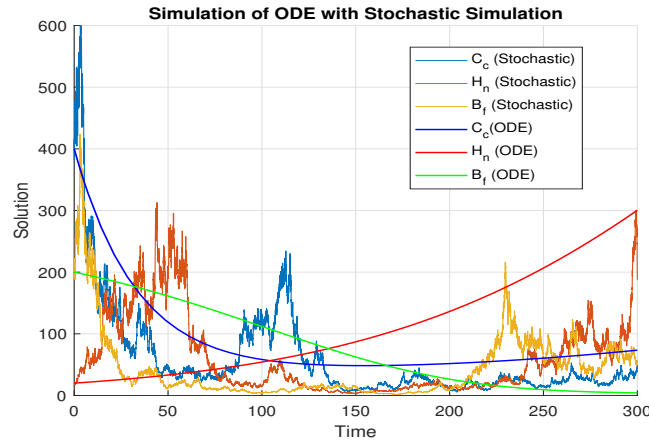Figure 7: Variation plot of concentration of CO_2 for the system (1) with and without human activities.

Figure 8: Stochastic and ODE variations for the system (10) for $\sigma_1 = 0.1, \sigma_2 = 0.15, \sigma_3 = 0.2$.

surface plots reflect that the atmospheric CO_2 can be reduced by reducing the anthropogenic emission rate and reduction rate of forest biomass. Figure (6) shows the global stability of X_{ie}. For the assigned parameters value, the condition of global stability is satisfied and so all the trajectories with different initial start converge to the unique interior equilibrium. Figure (7) shows the variation in the concentration of atmospheric carbon dioxide with and without human activities. It is clear from the figure that human activities contribute significantly in enhancing the level of atmospheric carbon dioxide and hence in the climate change. Thus to mitigate the climate change, the atmospheric level of CO_2 must be minimized, and that can be achieved if the human activities that contribute in emission of CO_2 gas are controlled or the growth of the human population is controlled. For the stochastic model, the Milstein's method is
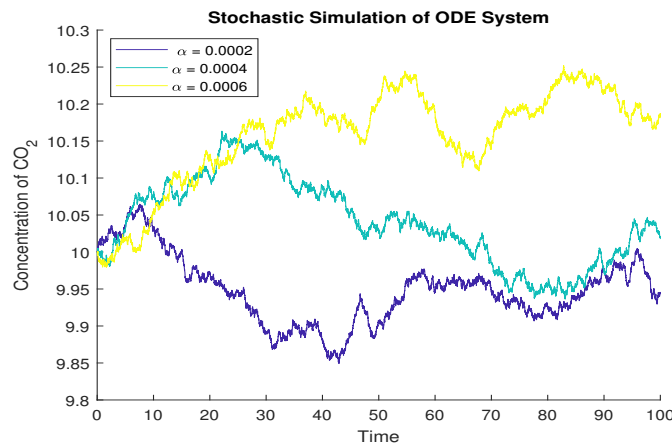

Figure 9: Stochastic variations of concentration of atmospheric CO_2 for different values of α for the system (10)for $\sigma_1 = 0.1, \sigma_2 = 0.15, \sigma_3 = 0.2$.

used to solve stochastic differential equation explained in [5]. Figure (8) shows the solution of the ordinary differential equation (ODE) system and its stochastic analogue. It ia clear from the figure that the stochastic fluctuation occurs around the equilibrium in the presence of small noise. Figures (9) and (10) show that the concentration of CO_2 increases (decreases) with the increase (decrease) of reduction rate of forest biomass as well as anthropogenic emission rate of CO_2.
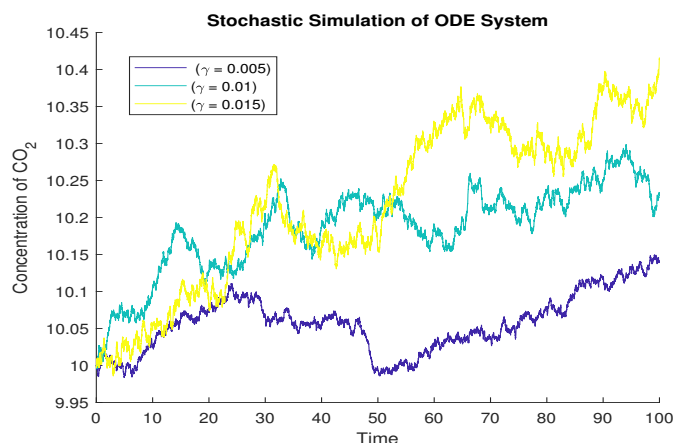
Figure 10: Stochastic variations of concentration of CO_2 for three different values of γ for the system (10) for $\sigma_1 = 0.1, \sigma_2 = 0.15, \sigma_3 = 0.2$.

6 Conclusion

This paper introduced and examined a nonlinear model designed to investigate the influence of the human population in a region on the dynamics of atmospheric CO_2, a significant factor contributing to climate change. The model formulation has considered various contributors to atmospheric CO_2 levels, encompassing anthropogenic emissions and natural sources such as volcanic eruptions and biological respiration. Additionally, the model takes into account the natural depletion of CO_2 through processes like photosynthesis and natural sinks. Two distinct non-negative equilibria arose within the proposed model: the human population free equilibrium and the interior equilibrium. Feasibility conditions for these equilibria were established, and their stability was thoroughly analyzed. Notably, the analysis highlighted the considerable impact of anthropogenic emissions and the reduction in forest biomass, driven by human population growth, on the concentration of CO_2. The study emphasized that curbing carbon dioxide emissions by controlling the anthropogenic emission rate and reduction rate of fossils fuels holds the potential to mitigate global warming and climate change effects. The findings underscored that the concentration of atmospheric CO_2 can be minimized by reducing the reduction rate of forest biomass and rate of anthropogenic emission, that can be achieved through measures such as minimizing deforestation for purposes like agriculture, infrastructure, and other human-related activities like burning of fossil fuels, fertilization, livestock production etc. Moreover, proficient management of human population growth is identified as a crucial element in mitigating CO_2 levels and addressing consequent impacts on climate change. This can be facilitated by lowering the reduction rate of forest biomass. Given the challenges posed by rapid population growth and urbanization, the reduction rate of forest biomass can be curbed to a certain extent. Therefore, it is recommended to counteract this trend by advocating the plantation of leafy trees throughout designated plantation avenues in the region. The model can be extended to other greenhouse gases. It can also be extended to four dimensional model by incorporating economic impact to mitigate CO_2 etc.

References

[1] Alexiadis, A., 2007, Global warming and human activity: A model for studying the potential instability of the carbon dioxide/temperature feedback mechanism, *Ecological Modelling*, 203(3-4), 243-256. DOI: https://doi.org/10.1016/j.ecolmodel.2006.11.020

[2] Dubey, B., 1997, Modelling the depletion and conservation of resources:effects of two interacting populations, *Ecological Modeling*, 101(1), 123-136. DOI: https://doi.org/10.1016/S0304-3800(97) 01974-1

[3] Dubey, B., and Narayanan, A. S., 2010, Modelling effects of industrialization, population and pollution on a renewable resource, *Nonlinear Analysis: Real World Applications*, 11(4), 2833-2848. DOI: `https://doi.org/10.1016/j.nonrwa.2009.10.007`

[4] Hale, J. K., 1969, *Ordinary Differential Equations*. John Wiley and Sons, New York.

[5] Higham, D. J., 2001, An algorithmic introduction to numerical simulation of stochastic differential equations, *SIAM review*, 43(3), 525-546. `https://doi.org/10.1137/S0036144500378302`

[6] Khan, M. M. H., Kramer, A., and Prufer-Kramer, L., 2011, Climate change and infectious diseases in megacities of the Indian subcontinent: A literature review, *Health in Megacities and Urban areas*, 135-152. DOI: `https://doi.org/10.1007/978-3-7908-2733-09`

[7] Misra, A. K., Lata, K., and Shukla, J. B., 2014, Effects of population and population pressure on forest resources and their conservation: a modeling study, *Environment, development and sustainability*, 16, 361-374. DOI: `https://doi.org/10.1007/s10668-013-9481-x`

[8] Misra, A. K. and Jha, A., 2021, Modeling the effect of population pressure on the dynamics of carbon dioxide gas, *Journal of Applied Mathematics and Computing*, 67(1-2), 623-640. DOI: `https://doi.org/10.1007/s12190-020-01492-8`

[9] Misra, A. K., and Jha, A., 2023, Modeling the role of renewable energy to mitigate the atmospheric level of carbon dioxide along with sustainable development, *Chaos: An Interdisciplinary Journal of Nonlinear Science*, 33(12). DOI: `https://doi.org/10.1063/5.0168714`

[10] Pachauri, R. K., Allen, M. R., Barros, V. R., Broome, J., Cramer, W., Christ, R., Church, J. A., Clarke, L., Dahe, Q., Dasgupta, P., and Dubash, N.K., 2014, Climate change 2014: synthesis report. *Contribution of Working Groups I, II and III to the fifth assessment report of the Intergovernmental Panel on Climate Change*, 151. Ipcc.

[11] Panja, P., 2021, Deforestation, Carbon dioxide increase in the atmosphere and global warming: A modelling study, *International Journal of Modelling and Simulation*, 41(3), 209-219. DOI: `https://doi.org/10.1080/02286203.2019.1707501`

[12] Shi, A., 2003, The impact of population pressure on global carbon dioxide emissions, 1975-1996: evidence from pooled cross-country data, *Ecological Economics*, 44(1), 29-42. DOI: `https://doi.org/10.1016/S0921-8009(02)00223-9`

[13] Tennakone, K., 1990, Stability of the biomass-carbon dioxide equilibrium in the atmosphere: mathematical model, *Applied Mathematics and Computation*, 35(2), 125-130. DOI: `https://doi.org/10.1016/0096-3003(90)90113-H`

[14] Woodwell, G. M., Hobbie, J. E., Houghton, R. A., Melillo, J. M., Moore, B., Peterson, B. J., and Shaver, G. R.,1983, Global deforestation: contribution to atmospheric carbon dioxide, *Science*, 222(4628), 1081-1086.

[15] Wu, X., Lu, Y., Zhou, S., Chen, L., and Xu, B., 2016, Impact of climate change on human infectious diseases: Empirical evidence and human adaptation, *Environment International*, 86, 14-23. DOI: `https://doi.org/10.1016/j.envint.2015.09.007`

[16] Yang, X., Chen, L., and Chen, J., 1996, Permanence and positive periodic solution for the single-species nonautonomous delay diffusive models, *Computers and Mathematics with Applications*, 32(4), 109-116. DOI: `https://doi.org/10.1016/0898-1221(96)00129-0`

[17] Trends in Atmospheric Carbon Dioxide, 2021, Global Monitoring Laboratory, *NOAA Research*. `https://gml.noaa.gov/ccgg/trends/global.html`